frontiers | Frontiers in Materials

TYPE Original Research
PUBLISHED 03 July 2023
DOI 10.3389/fmats.2023.1180745

OPEN ACCESS

EDITED BY
Pratheep K. Annamalai,
University of Southern Queensland, Australia

REVIEWED BY
Ang Lu,
Wuhan University, China
Jun-ichi Kadokawa,
Kagoshima University, Japan
Daniela Iannazzo,
University of Messina, Italy

*CORRESPONDENCE
Shih-Chen Shi,
scshi@mail.ncku.edu.tw
Tao-Hsing Chen,
thchen@nkust.edu.tw

RECEIVED 06 March 2023
ACCEPTED 16 June 2023
PUBLISHED 03 July 2023

CITATION
Shi S-C, Liu H-H, Chen T-H, Chen C-K and Ko B-T (2023), Preparation of aldehyde-graphene quantum dots from glucose for controlled release of anticancer drug.
Front. Mater. 10:1180745.
doi: 10.3389/fmats.2023.1180745

Preparation of aldehyde-graphene quantum dots from glucose for controlled release of anticancer drug

Shih-Chen Shi[1]*, Hsin-Hung Liu[1], Tao-Hsing Chen[2]*, Chih-Kuang Chen[3] and Bao-Tsan Ko[4]

[1]Department of Mechanical Engineering, National Cheng Kung University (NCKU), Tainan, Taiwan, [2]Department of Mechanical Engineering, National Kaohsiung University of Science and Technology (NKUST), Kaohsiung, Taiwan, [3]Department of Materials and Optoelectronic Science, National Sun Yat-sen University, Kaohsiung, Taiwan, [4]Department of Chemistry, National Chung-Hsing University, Taichung, Taiwan

In this study, we prepared graphene quantum dots (GQDs) via a green process using rice straw as a carbon source. The non-toxic nature of GQDs is suitable for application in human body-related research. Furthermore, GQDs possess biodegradability and biocompatibility characteristics, indicating high suitability for applications in the field of drug delivery. Based on the fact that acid-sensitive bonds between GQDs and the drug doxorubicin are formed by aldehyde groups on GQD surfaces, we adopted a semi-modified TEMPO method to partially oxidize the surface functional groups of GQDs without destroying the structure. This enabled an increase in the surface aldehyde group content, which in turn enhanced the drug loading capacity of GQDs. The aldehyde group content of the GQDs was measured via Fourier transform infrared (FTIR) spectroscopy, titration based on the Cannizzaro reaction, and X-ray photoelectron spectroscopy (XPS). The drug loading effect of the GQDs was determined via absorbance measurements at 485 nm on a UV-Vis spectrophotometer. The results indicated that the semi-modified TEMPO method significantly affected the introduction of surface aldehyde groups and the enhancement of the drug loading efficiency in GQDs. Finally, the polymeric material cationic poly (vinylcyclohexene carbonates) (CPVCHCs) was used for the encapsulation of GQDs and regulation of drug release. Under the premise that the total amount of drugs released remains unaffected, the initial burst release of the drug is effectively delayed, which aids in reducing harmful effects of the drug on the human body.

KEYWORDS

cellulose, circular economy, graphene quantum dot, drug delivery, drug release

1 Introduction

Lignocellulosic materials are organic compounds with the highest reserves on Earth and are mainly composed of cellulose, hemicellulose, and lignin in varying proportions. Given that they are naturally renewable and biodegradable, these types of materials are expected to be beneficial for humankind when used extensively (Anžlovar et al., 2016; Shi and Liu, 2021). Rice straw is a common agricultural waste product containing useful components such as cellulose and lignin. In recent years, the selective conversion of cellulose to multiple high-

value chemicals and high-quality fuels has become one of the most extensively studied areas in biomass research (Hu et al., 2014; Yabushita et al., 2014). The hydrolysis of cellulose to glucose is the starting point of all conversion processes; and development of techniques to enhance the efficiency of this process is highly significant. The techniques for the hydrolysis of cellulose to reduce sugars are mainly classified into enzymatic and acidic hydrolysis (Rorrer and Hawley, 1993; Pengfei et al., 2011). However, they have been gradually replaced by solid acid catalyst (SAC)-mediated hydrolysis owing to higher efficiency, lower cost, and greater simplicity. Furthermore, solid acids are readily separable from the reaction products and can be recycled and reused. This has evoked considerable research interest in various types of SACs (Vilcocq et al., 2014). The glucose obtained from cellulose hydrolysis is used as a raw material for the preparation of graphene quantum dots (GQDs) via hydrothermal synthesis.

Graphene is an emerging material with superior properties such as strength, and high electrical and thermal conductivity. Commonly used methods for graphene preparation include the Hummer's method, exfoliation, and hydrothermal synthesis (Razaq et al., 2022). GQDs correspond to a nanocarbon material that exhibits high electron mobility and luminescent properties—having attracted substantial interest in optoelectronics and biomedicine. With the advantages of low cytotoxicity, high biodegradability, and the ability to undergo surface modifications for realizing drug release via various types of triggers, GQDs exhibit high potential in future development of anticancer drug carriers (Mura et al., 2013). Different forms of surface modifications have been utilized in this field. In a study, folic acid was covalently bonded to the surfaces of nanoscale graphene oxide (nano GO). This was to specifically target Michigan Cancer Foundation-7 (MCF-7) breast cancer cells and form nanocarriers with high stability in the human body and target specific cells (Zhang et al., 2010). Various types of nanoparticles have also been used for temperature-controlled (Chen et al., 2013), magnetic field-controlled (Arias et al., 2011; Hua et al., 2011; Zhang et al., 2012), and voltage-controlled (Im et al., 2010; Yan et al., 2010; Kim et al., 2011) drug release.

There is a paucity of studies on methods for elevating the content of the aldehyde functional group on the surfaces of GQDs. However, such methods can realize increased drug loading and enhanced drug release effects. Researchers have reported that the use of perioxidate for the ring-opening oxidation of hydroxyl groups at C2 and C3 of cellulose to form aldehyde groups causes the destruction of the benzene ring structure of GQDs (Kim et al., 2000). In another study, it was observed that the separate bonding of graphene oxide (GO) with glyoxal (GLX), glutaraldehyde (GTA), and glyoxylic acid (GXA) did not cause the formation of independent aldehyde functional groups on GQDs (Chen et al., 2013). The TEMPO oxidation of cellulose [12] in the presence of sodium hypochlorite (NaClO), sodium bromide (NaBr), and an alkaline environment for preventing oxidation into esters has led to significant effects in the elevation of the aldehyde group content (Isogai et al., 2011). In another study, it was shown that encapsulation using the polymeric material cationic poly (vinylcyclohexene carbonates) (CPVCHCs) enabled the preparation of GQD nanocarriers. CPVCHCs possess high thermal stability, biodegradability, and abilities for gene attachment and delayed drug release. The encapsulation effectively increased the amount of loaded drug and delayed its burst release (Liu et al., 2021).

An important target of the application of GQDs in the field of drug delivery is the mass production of low-toxicity GQDs with drug release effects. In this study, we mainly focused on the use of a green material and green process for GQD production. Specifically, the green material corresponds to glucose obtained from the hydrolysis of rice straw-derived cellulose, whereas the green process corresponds to hydrothermal synthesis.

Based on this, we propose the following four hypotheses: 1) GQDs synthesized using the green raw material (cellulose) and green process (hydrothermal process) exhibit low biotoxicity; 2) the semi-modified TEMPO method is capable of realizing GQD surface aldehydation; 3) a higher amount of anticancer drugs can be loaded onto dehydration GQDs (GQD–CHO); 4) encapsulation using CPVCHCs effectively delays the initial burst release of the drug.

The aim of this study is to prepare GQDs that can realize high cell viability (≥80%) at high concentrations (≥400 μg/ml) for use as drug carriers in humans. Drug loading is dependent on the bonding between aldehyde functional groups on GQD surfaces and the anticancer drug. Thus, an increase in the surface aldehyde functional group content can be beneficial to the drug loading efficiency of GQDs. Increases in the low-toxicity GQD yield and drug loading efficiency enable the use of GQDs as carriers for the targeted delivery of anticancer drugs within the human body.

2 Materials and experiment

In this study, GQDs were prepared via the hydrothermal conversion of glucose obtained from the hydrolysis of rice straw-derived cellulose (Shi and Liu, 2021).

2.1 Materials

Glucose powder was obtained by converting cellulose extracted from rice straw in our laboratory.

The crystalline segment of cellulose is compact. Additionally, decomposing it directly into small glucose molecules is difficult. Therefore, first, a ball mill was used to grind it to destroy its crystalline segment. The rotating motion of the zirconia ball in the ball mill was used to grind the cellulose gradually. Second, the hydrothermal method formed a solid-state catalyst by the reaction of carbon powder and sulfuric acid. The ball-milled cellulose, catalyst, and water were then reacted at 200°C for 24 h to hydrolyze cellulose to glucose. In this process, the solid-state catalyst (sulfonated activated carbon catalyst) released weak acid; selectively hydrolyzed cellulose into glucose molecules; and then filtered through 0.22 μm filter paper to separate the aqueous glucose solution from the sulfonated activated carbon catalyst. TEMPO (2,2,6,6-Tetramethylpiperidine-1-oxyl) was used for the oxidation of GQDs to increase the aldehyde group content. CPVCHCs were prepared according to the process described by Liu et al. (2021).

2.2 Synthesis of GQDs from glucose via hydrothermal method

GQDs were obtained from the dehydration of the -OH and -H groups of glucose and other molecules in a hydrothermal environment. For the hydrothermal synthesis of GQDs, the following parameter combination for an optimum GQD yield was used. This combination was previously established by our laboratory: reaction time: 2 h; environment: argon atmosphere; temperature: 190°C; and concentration: 3 mg/ml. After reaction completion, the reaction products were filtered with a 0.22 μm syringe filter, centrifuged at 15,000 rpm for 30 min, and subjected to dialysis for 24 h for the removal of unreacted glucose molecules.

2.3 Analysis of GQD characteristics

The GQD sizes were measured via transmission electron microscopy (TEM). The chemical structure of the GQDs was determined via Fourier transform infrared (FTIR) spectroscopy (Thermo Nicolet NEXUS 470, GMI, Golden Valley, MN, United States). Special emphasis was placed on -OH at 3000–3500 cm^{-1}, -OH at 3000–3500 cm^{-1}, C-H at 2840 cm^{-1}, aromatic ring structure at 1600 cm^{-1}, -OH at 1400 cm^{-1}, and C-O at 1200 cm^{-1}. The graphene structure of the GQDs was analyzed via Raman spectroscopy.

2.4 Surface functionalization of GQDs and testing

The GQDs were subjected to functionalization for the elevation of the surface aldehyde group content. TEMPO (0.008 g) was added to 70 ml of GQD solution at 25°C. The mixture was subsequently stirred for 30 min, dialyzed for 1 d to remove the residual TEMPO, and freeze-dried for 36 h to obtain the GQD–CHO powder.

Subsequently, a titration experiment, which was designed based on the Cannizzaro reaction to determine the degree of substitution, was performed as follows:

- 10 ml of 0.02 M sodium hydroxide (NaOH) was added to 21 mg of GQD powder.
- This was followed by the sequential addition of 10 mL of 0.02 M sulfuric acid (H_2SO_4) and 0.3 ml of phenolphthalein.
- Finally, back titration was performed with an identical concentration of sodium hydroxide. The degree of substitution was calculated as follows:

$$\text{Degree of substitution} = \frac{C1*V1 - 2*C2*V2}{M*X}*10^6\ (\mu\text{mol/g}) \quad (1)$$

C1: NaOH concentration (M), C2: H_2SO_4 concentration (M).
V1: Volume of NaOH titrated (L),
V2: Volume of H_2SO_4 titrated (L).M: Mass of tested substance (g), X: Dryness (%) (X = 100% for freeze-dried samples).FTIR spectroscopy was performed again to determine the changes in the chemical structure after surface functionalization, and X-ray photoelectron spectroscopy (XPS, PHI VersaProbe 4, ULVAC-PHI, Japan) was utilized to analyze the changes in the component proportion at 287 eV.

2.5 Drug loading of GQD–CHO and measurement of the amount of loaded drug

Anticancer drug doxorubicin (DOX) and 10 mg of the freeze-dried GQD–CHO powder were dissolved and reacted in 10 ml of organic solvent dimethyl sulfoxide (DMSO). The reaction formed an imine bond between GQD–CHO and DOX, and released an HCl molecule. This caused acid sensitivity and fat solubility. Furthermore, 10 μl of triethylamine (TEA) was added for neutralization based on the calculated optimum volume ratio of DOX: TEA = 1:2. Subsequently, the reaction products were dialyzed and freeze-dried. The final DOX loading was calculated using the DOX calibration curve, combined with the absorption intensity, at 485 nm. This was measured using a UV spectrometer to determine the loading ratio and maximum amount of loaded drug.

2.6 CPVCHC encapsulation and testing

GHD–CHO was loaded with DOX (GQD–CHO–DOX) and encapsulated in CPVCHCs for protection. A schematic image for the preparation and chemical structures of CPVCHC is demonstrated in Figure 1. GQD–CHO–DOX (10 mg) powder and 10 mg of CPVCHC powder were separately dissolved in deionized water. The two solutions were subsequently mixed and stirred for 3 h to realize adequate mixing. Furthermore, TEM was adopted to measure the sizes of the synthesized drug carriers; and dynamic light scattering and zeta potential measurements were conducted to determine the changes in the surface potential and state of encapsulation. Finally, absorbance at 485 nm was measured over 48 h using a UV spectrometer. The drug release function and effects of different composite drug carriers in different environments were also investigated.

3 Results and discussion

3.1 Characterization of GQDs

The inset of Figure 2 is the TEM image, showing the appearance and size of a GQD prepared in this study. Sizes of the synthesized GQDs were 20–25 nm. When the graphene structures within the GQDs were analyzed via Raman spectroscopy, the D-band of amorphous carbon was observed at 1360 cm^{-1} and the G-band corresponding to the ordered carbon was observed at approximately 1537 cm^{-1}. The ratio of the intensities of the D- and G-bands (I_D/I_G) serves as a measure of the defect density of the graphene structure. High I_D/I_G values indicate high defect density within the material structure. The results indicate an I_D/I_G value of 0.9 for GQDs synthesized via the hydrothermal method.

In the FTIR spectra shown in Figure 3, the bands of O-H at 3400 cm^{-1}, C-H at 2840 cm^{-1}, aromatic ring vibrations at 1600 cm^{-1}, OH at 1400 cm^{-1}, and C-O at 1200 cm^{-1} corresponded to the -OH and -COOH functional groups on the GQDs. The spectrum of GQD–CHO lacks significant changes in the bands of O-H at 3400 cm^{-1}, C-H at 2840 cm^{-1}, aromatic ring vibrations at 1600 cm^{-1}, and the C-O bond at

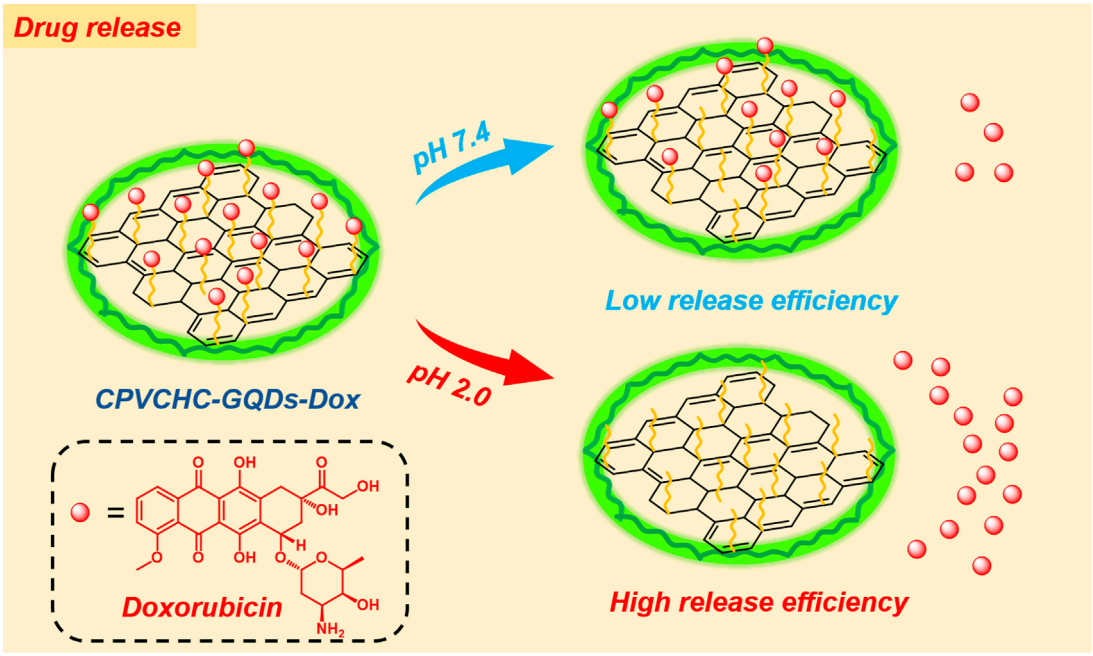

FIGURE 1
Schematic image for the preparation and chemical structure of CPVCHC.

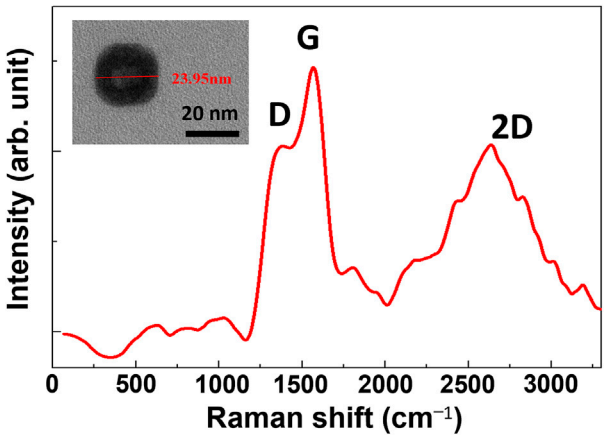

FIGURE 2
Raman analysis of GQDs (Inset: TEM image of a GQD).

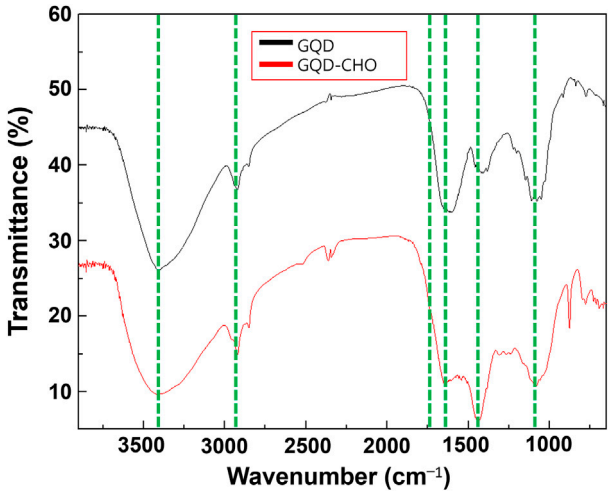

FIGURE 3
FTIR analysis of GQDs.

1200 cm^{-1}. Following the oxidation of -OH to -CHO and -COOH, the appearance of a peak was observed at approximately 1740 cm^{-1}, corresponding to the C=O bond of the aldehyde functional group. The aldehydation effect is positively correlated with the peak intensity. However, the FTIR spectrum obtained in this study merely exhibited an inconspicuous peak corresponding to the aldehyde functional group. Therefore, the presence of aldehyde groups and increase in their proportion after aldehydation were further demonstrated by the calculation of the degree of substitution and XPS analysis.

3.2 Measurement of aldehydation effect

The titration experiment was performed thrice for the GQDs oxidized via the semi-modified TEMPO method and unoxidized GQDs, and the average values for both types of GQDs were calculated and compared to determine the increase in the degree of substitution and the proportion of increase. As illustrated in Table 1, the average increase in the degree of substitution was 42.0%,

TABLE 1 Analysis of aldehyde group content via titration experiment.

Unit: μmol/g	1st titration	2nd titration	3rd titration	Average
TEMPO oxidation	1904.7	1785.7	1964.3	1885
Untreated	1371.4	1297.5	1311.2	1327

Proportion of increase in degree of substitution determined by Cannizzaro reaction-based titration (%)
42.0

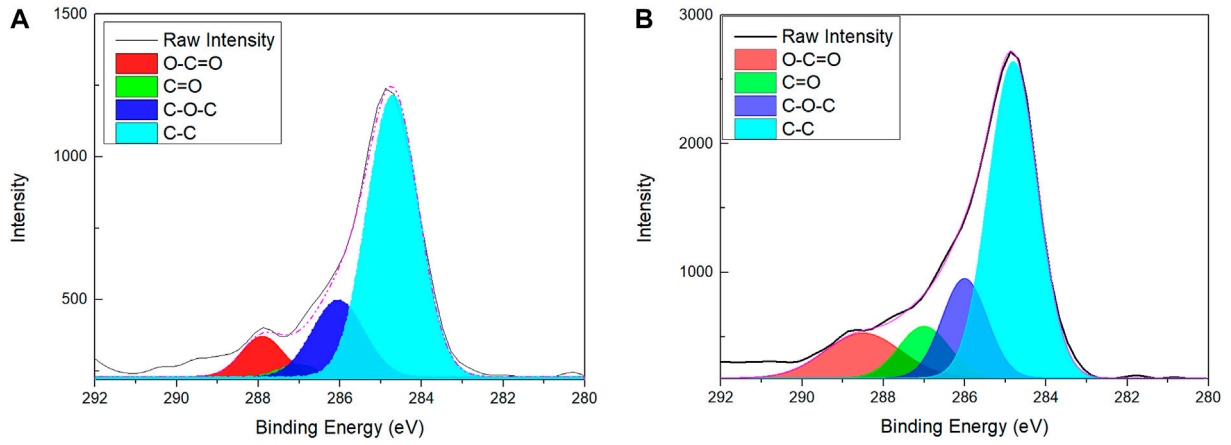

FIGURE 4
XPS analysis of **(A)** as-grown GQDs and **(B)** GQD–CHO.

TABLE 2 Results of XPS analysis.

	Bonding ratio (%)			
	O-C=O	C=O	C-O-C	C-C
As-grown GQDs	8.1	2.3	19.4	70.0
GQD–CHO	13.1	9.9	17.1	60.0

which indicates the realization of superior aldehydation effects. In addition to being proven as a successful oxidation method via FTIR spectroscopy, the semi-modified TEMPO oxidation method demonstrated effects in the addition of the aldehyde functional groups.

Considering that certain errors exist in the titration measurement of degree of substitution by the aldehyde groups, we performed elemental analysis of GQDs via XPS analysis (Figure 4). The XPS spectrum of untreated (as-grown) GQDs in Figure 4A clearly shows the presence of bands for the C-C bond, O-C=O carboxylic acid group, and C-O-C epoxy group. Furthermore, the results showed that aldehyde groups merely accounted for a small proportion (2.25%) of the as-grown GQDs. Figure 4B shows the XPS spectrum of GQDs subjected to oxidation via the semi-modified TEMPO method. To realize the termination of oxidation at the aldehyde stage and prevent further oxidation to carboxylic aid groups or ester groups—Which are the final products of the original TEMPO method—We modified the TEMPO method by omitting the addition of NaClO. XPS analysis, performed after the oxidation reaction, revealed that the proportions of carboxylic acid and aldehyde groups were elevated (9.9%). The proportions of various types of bonds listed in Table 2 show that superior effects are obtained in the elevation of the relative proportion. The proportion of carboxylic groups was also increased. When these results are considered with the results of FTIR spectroscopy (oxidation effect) and titration of the degree of the aldehyde group substitution (elevation of aldehydate group content), it can be preliminarily concluded that a certain proportion of the aldehyde groups was inevitably oxidized to carboxylic acid groups despite the non-addition of NaClO. This was evident from the increase in the carboxylic acid group content shown via FTIR spectroscopy and XPS analysis. However, the titration measurement of the degree of substitution and XPS elemental analysis demonstrated that the oxidation method can still realize solid effects in elevating the aldehyde content.

3.3 Drug loading effect

To determine the amounts of loaded drugs, the measurements of the absorbance of DOX at 485 nm were first obtained via ultraviolet-visible light (UV-vis) spectroscopy. It was used for plotting the calibration curve shown in Figure 5A. Subsequently, the calibration curve was used to derive the amount of DOX successfully grafted to

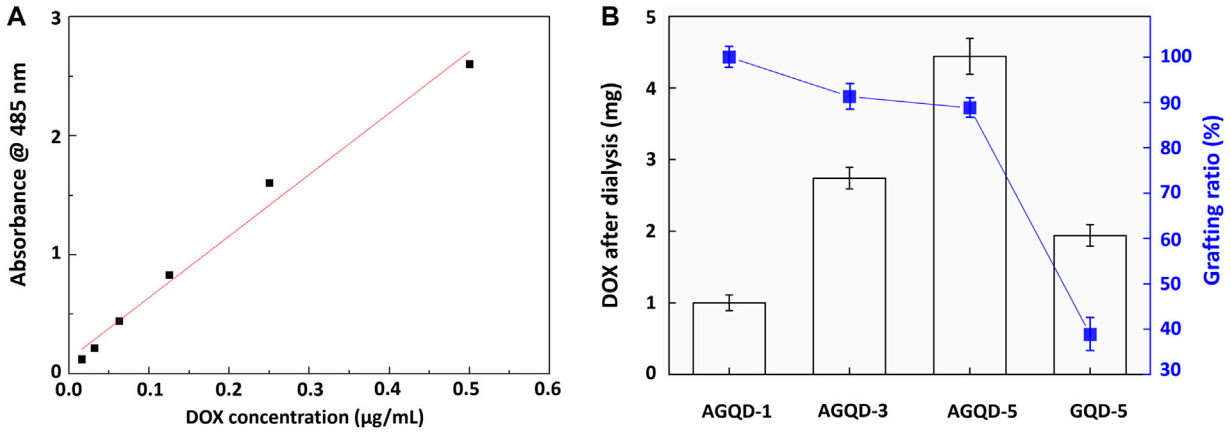

FIGURE 5
(A) DOX dose and calibration line of absorption spectrum and **(B)** DOX weight and grafting ratio on GQD.

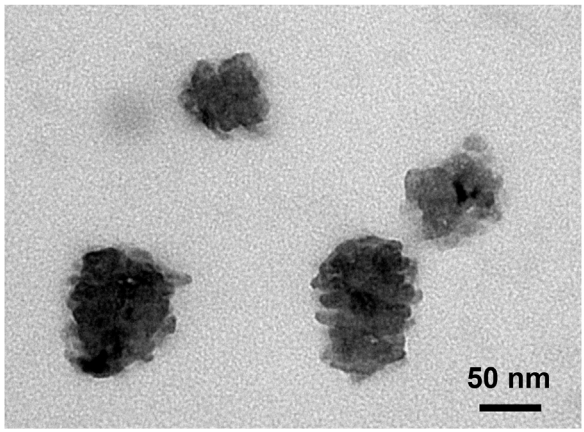

FIGURE 6
TEM image of GQD–DOX–CPVCHC.

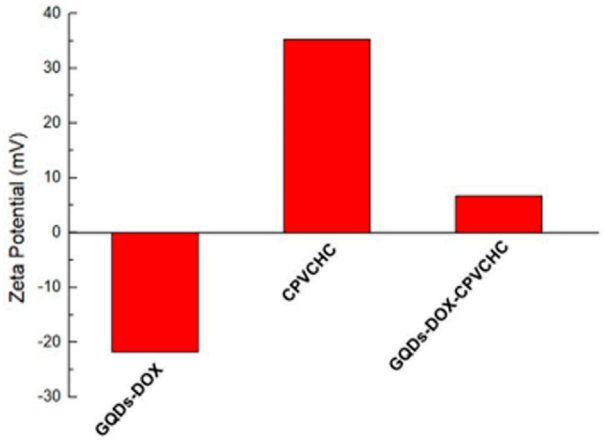

FIGURE 7
Zeta potential analysis of GQD, CPVCHCs, and GQD–DOX–CPVCHC.

the samples under conditions of different parameter values, as shown in Figure 5B. It can be observed that GQD–CHO and as-grown GHQs exhibited relatively higher amounts of loaded drug.

3.4 Observation of CPVCHC-encapsulated GQDs

GQDs encapsulated by the polymeric CPVCHC material (GQD–DOX–CPVCHC) were observed via TEM and fluorescence microscopy. In the TEM image of GQD–DOX–CPVCHC shown in Figure 6, the diameters of the polymeric composite GQDs are in the range of 50–100 nm. That is, higher than that of the as-grown GQDs.

The zeta potentials of GQD–DOX, CPVCHCs, and GQD–DOX–CPVCHC were subsequently measured. As shown in Figure 7, the surface potential values are −21.81, 35.28, and 6.68 mV, respectively. After the adsorption of the negatively-charged GQD–DOX, the positive surface potential of CPVCHCs was considerably reduced. This demonstrated that GQD–DOX was adequately encapsulated by CPVCHCs.

3.5 Measurement of drug release

Figure 8 compares the drug release curves of the polymeric composite drug carrier. A higher amount of drug was released at pH 5.5 than at neutral pH of 7.4, because acid-sensitive bonds between DOX and GQDs are prone to breakage in the presence of a weakly acidic environment near the tumor cells.

Figure 9 shows the drug release curves of DOX grafted onto aldehydated and non-aldehydated GQDs. Furthermore, aldehydated and non-aldehydated GQDs exhibit better drug

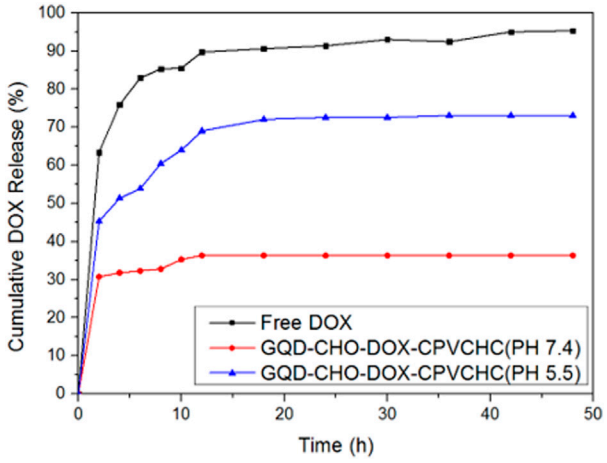

FIGURE 8
Drug release curves of GQD–DOX–CPVCHC composites.

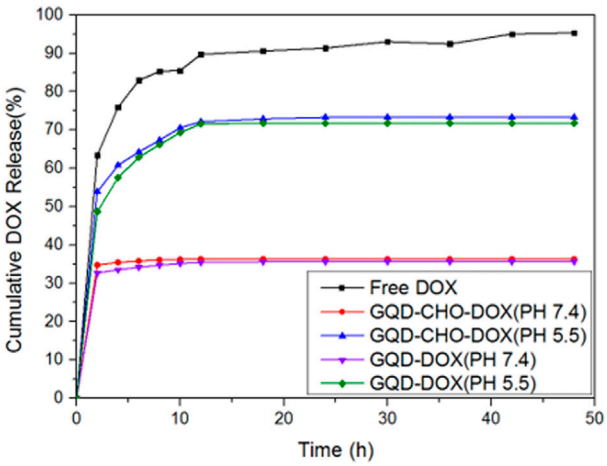

FIGURE 9
Drug release curves of GQD–DOX composites.

release and almost identical release rates in the weakly acidic environment. The purpose of aldehyde bonding was to increase the drug loading, as shown in Figure 4B. Taking the 24th hour at pH 5.5 as an example, the release rate of GQD-CHO-DOX/GQD-DOX was 73.3%/71.75%, and the grafted amount of DOX (5 mg in this experiment) was 4.44 mg/1.94 mg. Therefore, the release ratio at 24 h should have been 3.25 mg/1.39 mg. Therefore, in the case of quantitative GQD treatment, the total amount of DOX that the hydroformylated GQD could release was 2.29 times that of the original in the same period.

Figure 10 shows the drug release curves of GQDs with and without CPVCHC encapsulation in identical environments. Encapsulated GQDs showed significant effects in the delay of the initial burst release of the drug. This can prevent the early release of excessively high amounts of drugs into the bloodstream. However,

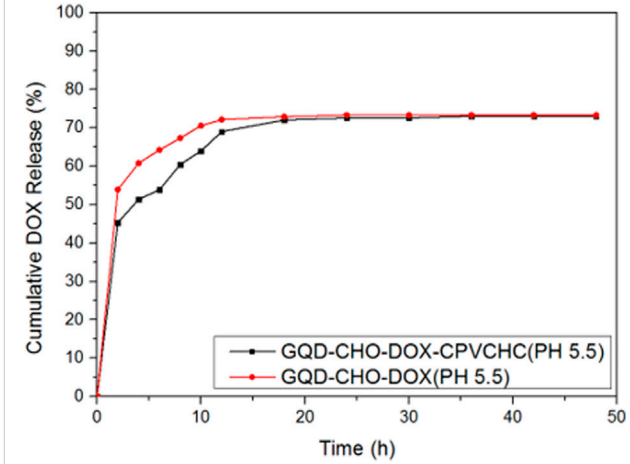

FIGURE 10
Drug release curves of GQDs with and without CPVCHC encapsulation.

the total amount of drug released was comparable to that of the unencapsulated GQDs.

4 Conclusion

This study demonstrated the method of preparing GQD from cellulose and the role of GQD as an anticancer drug carrier. GQDs were prepared using a green raw material and a green process. This demonstrated the extremely low biotoxicity of green GQDs. Subsequently, a semi-modified TEMPO method was adopted to increase the surface aldehyde functional group content of the prepared GQDs. Measuring the degree of substitution and XPS analysis indicated that aldehyde group content was significantly increased. Furthermore, it was determined that the addition of aldehyde groups simultaneously increased the amount of drugs that could be loaded. This demonstrated the enhancement of the drug loading efficiency of GQDs when used as drug carriers.

The results of the drug release experiment revealed that CPVCHC encapsulation does not reduce the total amount of drug released and drug release efficiency after the initial burst release. The encapsulation also delays the release of the drug before reaching the target cells. Therefore, the findings of this study provide a scientific basis for the future development of CPVCHC-encapsulated composite GQDs. They comprise a higher proportion of aldehyde groups and exhibit immense potential for applications in the field of drug loading and delivery.

Cellulose is derived from agricultural waste. This is more in line with energy conservation and carbon reduction than the traditional use of incineration to treat agricultural waste and convert it into a valuable resource. The bio-resourced carbons made of natural polymer cellulose as raw materials, and natural processes, also have the characteristics of simple operation and biocompatibility. Therefore, they are more suitable for applied biology. Furthermore,

natural polymer materials have biodegradability characteristics, and will not affect the environment in subsequent recycling treatment. A circular economy based on cellulose can be realized.

Data availability statement

The original contributions presented in the study are included in the article/supplementary material, further inquiries can be directed to the corresponding author.

Author contributions

S-CS and T-HC, Funding acquisition, Supervision, Writing—Review and editing; H-HL, Investigation Formal analysis, and Writing—Original draft; C-KC and B-TK: resources. All authors contributed to the article and approved the submitted version.

Funding

This work was supported by the National Science and Technology Council, Taiwan (grant number MOST 110-2221-E-006-150, 111-2221-E-006-145, 111-2221-E-006-147-MY2, and 111-2221-E-006-133, 111-2628-E-992-001-MY2).

Acknowledgments

The authors gratefully acknowledge the use of EM000700 of MOST 110-2731-M-006-001 belonging to the Core Facility Center of National Cheng Kung University.

Conflict of interest

The authors declare that the research was conducted in the absence of any commercial or financial relationships that could be construed as a potential conflict of interest.

Publisher's note

References

Anžlovar, A., Huskić, M., and Žagar, E. (2016). Modification of nanocrystalline cellulose for application as a reinforcing nanofiller in PMMA composites. *Cellul* 23, 505–518. doi:10.1007/s10570-015-0786-9

Arias, J. L., Reddy, L. H., Othman, M., Gillet, B., Desmaële, D., Zouhiri, F., et al. (2011). Squalene based nanocomposites: A new platform for the design of multifunctional pharmaceutical theragnostics. *ACS Nano* 5, 1513–1521. doi:10.1021/nn1034197

Chen, K.-J., Liang, H.-F., Chen, H.-L., Wang, Y., Cheng, P. Y., Liu, H. L., et al. (2013). A thermoresponsive bubble-generating liposomal system for triggering localized extracellular drug delivery. *ACS Nano* 7, 438–446. doi:10.1021/nn304474j

Hu, L., Wu, Z., Xu, J., Sun, Y., Lin, L., and Liu, S. (2014). Zeolite-promoted transformation of glucose into 5-hydroxymethylfurfural in ionic liquid. *Chem. Eng. J.* 244, 137–144. doi:10.1016/j.cej.2014.01.057

Hua, M.-Y., Liu, H.-L., Yang, H.-W., Chen, P. Y., Tsai, R. Y., Huang, C. Y., et al. (2011). The effectiveness of a magnetic nanoparticle-based delivery system for BCNU in the treatment of gliomas. *Biomaterials* 32, 516–527. doi:10.1016/j.biomaterials.2010.09.065

Im, J. S., Bai, B. C., and Lee, Y.-S. (2010). The effect of carbon nanotubes on drug delivery in an electro-sensitive transdermal drug delivery system. *Biomaterials* 31, 1414–1419. doi:10.1016/j.biomaterials.2009.11.004

Isogai, A., Saito, T., and Fukuzumi, H. (2011). TEMPO-oxidized cellulose nanofibers. *nanoscale* 3, 71–85. doi:10.1039/C0NR00583E

Kim, H., Jeong, S.-M., and Park, J.-W. (2011). Electrical switching between vesicles and micelles via redox-responsive self-assembly of amphiphilic rod– coils. *J. Am. Chem. Soc.* 133, 5206–5209. doi:10.1021/ja200297j

Kim, U.-J., Kuga, S., Wada, M., Okano, T., and Kondo, T. (2000). Periodate oxidation of crystalline cellulose. *Biomacromolecules* 1, 488–492. doi:10.1021/bm0000337

Liu, G.-L., Wu, H.-W., Lin, Z.-I., Liao, M. G., Su, Y. C., Chen, C. K., et al. (2021). Synthesis of functional CO 2-based polycarbonates via dinuclear nickel nitrophenolate-based catalysis for degradable surfactant and drug-loaded nanoparticle applications. *Polym. Chem.* 12, 1244–1259. doi:10.1039/D0PY01755H

Mura, S., Nicolas, J., and Couvreur, P. (2013). Stimuli-responsive nanocarriers for drug delivery. *Nat. Mat.* 12, 991–1003. doi:10.1038/nmat3776

Pengfei, Y., Kobayashi, H., and Fukuoka, A. (2011). Recent developments in the catalytic conversion of cellulose into valuable chemicals. *Chin. J. Catal.* 32, 716–722. doi:10.1016/S1872-2067(10)60232-X

Razaq, A., Bibi, F., Zheng, X., Papadakis, R., Jafri, S. H. M., and Li, H. (2022). Review on graphene-graphene oxide-reduced graphene oxide-based flexible composites: From fabrication to applications. *Mater* 15, 1012. doi:10.3390/ma15031012

Rorrer, G. L., and Hawley, M. C. (1993). Vapor-phase HF solvolysis of cellulose: Modification of the reversion oligosaccharide distribution by *in-situ* methanolysis. *Carbohydr. Polym.* 22, 9–13. doi:10.1016/0144-8617(93)90160-6

Shi, S.-C., and Liu, G.-T. (2021). Cellulose nanocrystal extraction from rice straw using a chlorine-free bleaching process. *Cellul* 28, 6147–6158. doi:10.1007/s10570-021-03889-5

Vilcocq, L., Castilho, P. C., Carvalheiro, F., and Duarte, L. C. (2014). Hydrolysis of oligosaccharides over solid acid catalysts: A review. *ChemSusChem* 7, 1010–1019. doi:10.1002/cssc.201300720

Yabushita, M., Kobayashi, H., and Fukuoka, A. (2014). Catalytic transformation of cellulose into platform chemicals. *Appl. Catal. B* 145, 1–9. doi:10.1016/j.apcatb.2013.01.052

Yan, Q., Yuan, J., Cai, Z., Xin, Y., Kang, Y., and Yin, Y. (2010). Voltage-responsive vesicles based on orthogonal assembly of two homopolymers. *J. Am. Chem. Soc.* 132, 9268–9270. doi:10.1021/ja1027502

Zhang, L., Wang, T., Yang, L., Liu, C., Wang, C., Liu, H., et al. (2012). General route to multifunctional uniform yolk/mesoporous silica shell nanocapsules: A platform for simultaneous cancer-targeted imaging and magnetically guided drug delivery. *Chem. Eur. J.* 18, 12512–12521. doi:10.1002/chem.201200030

Zhang, L., Xia, J., Zhao, Q., Liu, L., and Zhang, Z. (2010). Functional graphene oxide as a nanocarrier for controlled loading and targeted delivery of mixed anticancer drugs. *small* 6, 537–544. doi:10.1002/smll.200901680